Journal of the Serbian Chemical Society
JSCS-info@shd.org.rs • www.shd.org.rs/JSCS
J. Serb. Chem. Soc. *83* (2) 139–155 (2018)
JSCS–5064
UDC 547.588.21:544.032.732+519.677
Original scientific paper

Experimental and theoretical study on solvent and substituent effects on the intramolecular charge transfer in 3-[(4--substituted)phenylamino]isobenzofuran-1(3*H*)-ones

NEVENA Ž. PRLAINOVIĆ[1#], MILICA P. RANČIĆ[2#], IVANA STOJILJKOVIĆ[2], JASMINA B. NIKOLIĆ[3*#], SAŠA Ž. DRMANIĆ[3#], ISMAIL AJAJ[4] and ALEKSANDAR D. MARINKOVIĆ[3#]

[1]*Innovation Center, Faculty of Technology and Metallurgy, Karnegijeva 4, 11120 Belgrade, Serbia,* [2]*Faculty of Forestry, University of Belgrade, Kneza Višeslava 1, 11030 Belgrade, Serbia,* [3]*Faculty of Technology and Metallurgy, University of Belgrade, Karnegijeva 4, 11120 Belgrade, Serbia and* [4]*Faculty of Arts and Science, The University of El-Margeb, Mesallata, Libya*

(Received 8 April, revised 28 November, accepted 7 December 2017)

Abstract: The substituent and solvent effects on solvatochromism in 3-[(4-substituted)phenylamino]isobenzofuran-1(3*H*)-ones were studied using experimental and theoretical methodologies. The effect of specific and non-specific solvent–solute interactions on the shifts of UV–Vis absorption maxima were evaluated using the Kamlet–Taft and Catalán solvent parameter sets. The experimental results were studied by density functional theory (DT) and time-dependent density functional theory (TD-DFT). The HOMO/LUMO energies (E_{HOMO}/E_{LUMO}) and energy gap (E_{gap}) values, as well as the mechanism of electronic excitations and the changes in the electron density distribution in both ground and excited states of the investigated molecules were studied by calculation in the gas phase. The electronic excitations were calculated by the TD-DFT method in the solvent methanol. It was found that both substituents and solvents influence the degree of π-electron conjugation of the synthesized molecules and affect the intramolecular charge transfer character.

Keywords: phthalides; solvatochromism; substituent effect; LSER; quantum chemical calculation.

INTRODUCTION

Phthalides or 3*H*-isobenzofuran-1-ones represent a widespread group of secondary metabolites in plants, responsible for numerous pharmacological properties and biological activities. To date, all known natural phthalide compounds have been identified as derivatives of 3*H*-isobenzofuran-1-one.[1] Phthalides are

* Corresponding author. E-mail: jasmina@tmf.bg.ac.rs
# Serbian Chemical Society member.
https://doi.org/10.2298/JSC170408003P

characterized by a bicyclic core (Scheme 1), derived from the fusion of a γ-lactone with benzene. They are considered internal esters of the corresponding γ-hydroxy carboxylic acids. Although the occurrence of the parent phthalide (3*H*--isobenzofuran-1-one) in natural products dates back to the 18th century, interest for a wide range of biological activities of its diverse derivatives has only recently arisen in the scientific community.[2]

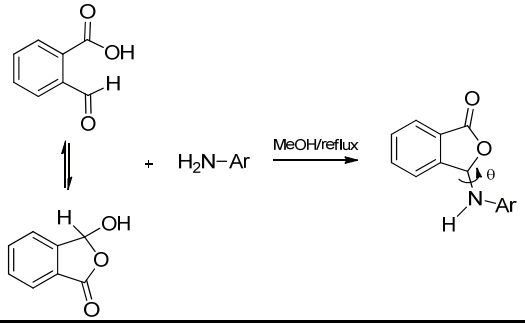

Compound	Ar	Compound	Ar
1	Phenyl	**6**	4-Chlorophenyl
2	4-Methylphenyl	**7**	4-Acetylphenyl
3	4-Methoxyphenyl	**8**	4-Nitrophenyl
4	4-Hydroxyphenyl	**9**	2-Pyridyl
5	4-Fluorophenyl	**10**	3-Pyridyl

Scheme 1. General procedure for the synthesis of 3-[(4-substituted)phenylamino]isobenzofuran-1(3*H*)-ones.

Phthalide are also versatile starting materials and key intermediates for the synthesis of a variety of natural products.[3] For example, 3-arylphthalides are intermediates for the synthesis of tri- and tetracyclic natural products, such as anthracycline antibiotics.[2] Various chemical modifications of this heterocycle have resulted in compounds with a wide spectrum of biological activities, *e.g.*, antibacterial,[4] antitubercular,[5] antifungal,[6] anti-HIV,[7] anti-oxidant,[8] antitumor and immunosuppressive activity.[9] Although phthalides have been components of traditional medicines from ancient times, the diverse range of their therapeutic activities has only recently attracted the attention of scientists.[2] The success of *n*-butylphthalide (NBP),[3] which is currently on the market as an antiplatelet drug for ischemia–cerebral apoplexy, has led to the development of phthalides as a class of pharmaceutically important natural products. It was also approved, by the state food and drug administration of China in 2002, as an anti-ischemic stroke drug. It inhibits platelet aggregation, improves microcirculation, and mitigates ischemic brain injury.[2] However, most of the recent studies have dealt with 3-substituted phthalides due to their wide range of pharmacological applic-

ations. Hitherto, studies on the structure and activity relationships have been limited to NBP.[3]

However, previous literature data indicate that several molecular properties, particularly electronic properties, usually correlate with their biological activity and hence, it could be noted that future prospects for the design and development of new biologically active molecules are based on the correlation between theoretical and experimental properties. The photophysical properties of molecules are mainly governed by the polarity of the medium, hydrogen bonding and electronic substituent effects.[10,11]

In the present work, a series of 3-[(4-substituted)phenylamino]isobenzofuran-1(3*H*)-ones was synthesized in order to study the influence of solvent––solute interactions on the shifts in UV spectra. Interactions with the solvent were investigated using linear solvation energy relationships (LSER). The effects of solvent dipolarity/polarizability and solvent–solute hydrogen bonding interactions were evaluated by means of the LSER model of Kamlet–Taft, Eq. (1):[12,13]

$$\nu_{\max} = \nu_0 + s\pi^* + b\beta + a\alpha \quad (1)$$

where $\nu_{\max}$ is the absorption maxima frequency positions, π^* is an index of the solvent dipolarity/polarizability; β is a measure of the solvent hydrogen-bond acceptor (HBA) basicity; α is a measure of the solvent hydrogen-bond donor (HBD) acidity, and ν_0 is the maximum position value in cyclohexane as reference solvent. The regression coefficients s, b and a in Eq. (1) measure the relative susceptibilities of the absorption frequencies to the solvent effect.

The effects of solvent dipolarity, polarizability and solvent–solute hydrogen bonding interactions were evaluated by means of the linear solvation energy relationship (LSER) model of Catalán,[14] given by Eq. (2):

$$\nu_{\max} = \nu_0 + aSA + bSB + cSP + dSdP \quad (2)$$

where *SA*, *SB*, *SP* and *SdP* characterize acidity, basicity, polarizability and dipolarity of a solvent, respectively; and *a* to *d* are the regression coefficients describing the sensitivity of the absorption maximum to the different types of solvent––solute interactions. The separation of non-specific solvent effects, term π^* in Eq. (1), into two terms: dipolarity and polarizability, *SP* and *SdP* in Eq. (2), contributes to advantageous analysis of the solvatochromism of the studied compounds. The solvent parameters used in Eq. (1) are given in Tables S-I and S-II of the Supplementary material to this paper.

The physicochemical properties of 3-[(4-substituted)phenylamino]isobenzofuran-1(3*H*)-ones (Scheme 1) were investigated using both experimental and theoretical methodologies. The computational studies included geometry optimization by density functional theory calculations (DFT) and time-dependent density functional theory calculations (TD-DFT) of electronic transitions.[15]

EXPERIMENTAL

Materials

All chemicals used in this study were reagent grade or *p.a*. quality, and used as received. Phthalaldehydic acid, aniline, glacial acetic acid, 4-methylaniline, 4-methoxyaniline, 4-hydroxyaniline, 4-fluoroaniline, 4-chloroaniline, 4-nitroaniline, 4-acetylaniline, 2-aminopyridine and 3-aminopyridine were purchased from Sigma–Aldrich. All used solvents were of spectroscopic quality (Table S-I of the Supplementary material to this paper).

*General procedure for the synthesis of 3-[(4-substituted)phenylamino]isobenzofuran-1(3*H*)-ones*

A solution of 5 mmol of aniline or an aniline derivative in 10 mL methanol was refluxed with phthalaldehydic acid (0.75 g, 5.0 mmol) for 3 h in the presence of a few drops of acetic acid. The obtained product was collected by filtration, air dried and recrystallized from ethanol. The structures and the numbering of the synthesized compounds are given in Table S-III of the Supplementary material.

Characterization methods

The ^{1}H- and ^{13}C-NMR spectral measurements were realised on a Varian Gemini 200 spectrometer. The spectra were recorded at room temperature in deuterated dimethyl sulphoxide (DMSO-d_6) at ambient temperature. The chemical shifts are expressed in ppm values referenced to TMS (δ_H = 0 ppm) for the ^{1}H-NMR spectra, and the residual solvent signal (δ_C = = 39.5 ppm) for ^{13}C-NMR spectra. The FT-IR spectra were recorded on a Nicolet iS10 spectrometer (Thermo Scientific) using the ATR method. Elemental analyses (C, H, N and O) were performed using a Vario EL III elemental analyzer, and the F and Cl contents were calculated by subtraction.

The UV absorption spectra were measured in the range 200–600 nm using a Shimadzu 1700 UV–Vis spectrophotometer. The UV–Vis spectra were taken in spectroscopic quality solvents (Fluka) at a concentration of 1×10^{-5} mol dm^{-3}. Three measurements were performed and mean value is presented.

Theoretical calculations

Geometries of all molecular species were optimized by the DFT method using the B3LYP/6-31G(d,2p) basis set. In order to find the global minimum on the potential energy surface, multiple geometry optimizations were performed for every compound, with varying rotatable torsion angles (θ, Scheme 1) in increments of 30° and minimizing the energy with respect to all geometrical parameters. The nature of the lowest energy minimum was further confirmed with frequency calculations; no negative frequencies were found.

The theoretical absorption spectra and ground/excited state properties were calculated on the DFT/B3LYP/6-31G(d,2p)-optimized geometries using TD-DFT. The TD-DFT calculations were realised in methanol with the CAM-B3LYP long range corrected functional[15] and the 6-31G(d,p) basis set. The solvent in the TD-DFT calculations was simulated with the polarizable continuum model (PCM). All quantum chemical calculations were performed using the Gaussian 09 program package.[16]

RESULTS AND DISCUSSION

*Effects of solvents on the absorption spectra of 3-[(4-substituted)phenylamino]-isobenzofuran-1(3*H*)-ones*

Phthalaldehydic acid is often represented as having an aldehyde and acid group. However, based on spectroscopic data, it is obvious that, depending on the

solvent and temperature, phthalaldehydic acid exists in both, an open and ring form structure.[17] The open and ring form structures are presented in Scheme 1. The reaction of phthalaldehydic acid with aniline was described previously.[18] The 3-anilino phthalide was the only product obtained by refluxing the reaction mixture for 3 h in methanol as the solvent.

The study of the solvent effects on the absorption spectra of organic compound allows access to some fundamental molecular properties.[12,18,20] One of the general concepts concerning the relationship between molecular structure and absorption spectrum leads to conclusion that the existence of planarity in the molecular geometry produces higher bathochromic shifts in the UV–Vis spectra due to increased π-conjugation throughout the investigated molecules.[21] In order to study the influence of solvent–solute interactions on the absorption maxima, the UV–Vis spectra of ten synthesized 3-[(4-substituted)phenylamino]isobenzofuran-1(3*H*)-ones were recorded in sixteen solvents of different properties. Characteristic spectra in dichloromethane and methanol are shown as examples in Fig. 1. From the presented UV–Vis spectra (Fig. 1), a diversity of the spectra with two main bands could be noticed. The first band appears in the range from 215–225 nm, and the other in the range from 275–285 nm with the exception of compound **8** that appears at 330 nm. It could be observed that both the position and intensity of the main absorption bands, presented in Tables I and II, depend on the electronic structure of compounds and the solvent properties. The data from Tables I and II indicate that the values of the absorption frequencies of the investigated compounds depend on the substituent and the solvent effect, although the absorption bands of both electron-donor and electron-acceptor-substituted derivatives appear at similar wavelengths (in the range 10–20 nm) compared to those for the unsubstituted compound **1**.

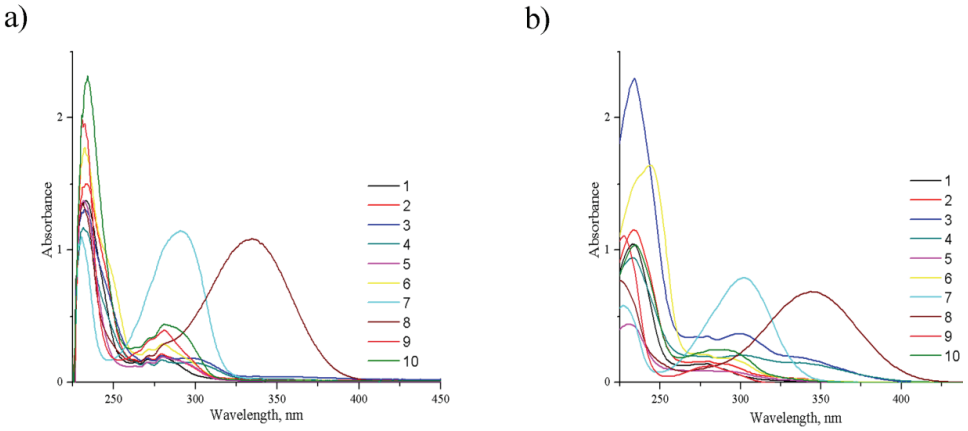

Fig. 1. Absorption spectra of compounds **1**–**10** in solvent a) dichloromethane and b) methanol.

TABLE I. Absorption frequencies ($\nu_{max}\times10^{-3}$ / cm^{-1}) for the lower wavelength peak of 3-[(4-substituted)phenylamino]isobenzofuran-1(3*H*)-ones in selected solvents

Solvent	Substituent									
	1	**2**	**3**	**4**	**5**	**6**	**7**	**8**	**9**	**10**
1,2-Dichloroethane	42.92	41.67	42.92	42.92	43.10	43.86	43.86	41.15	44.25	42.74
Decan-1-ol	42.74	42.74	42.37	42.92	43.10	48.78	43.20	42.70	44.05	42.74
Dichloromethane	42.92	42.74	42.92	43.20	43.20	43.29	43.48	42.91	43.48	42.74
1,4-Dioxane	42.28	42.92	42.19	42.92	43.01	43.48	43.29	40.98	43.10	42.83
Ethane-1,2-diol	42.19	42.37	43.29	42.74	42.55	43.67	42.92	40.16	43.48	42.74
Ethanol	42.74	42.92	42.74	43.10	43.29	44.25	43.86	41.15	44.05	42.55
Water	43.48	42.64	42.92	42.37	43.53	44.37	43.83	40.98	43.67	42.92
Hexane	43.38	43.29	42.74	42.84	43.48	44.64	44.64	41.49	44.64	43.48
2-Methylpropan-1-ol	42.74	42.64	42.92	42.83	43.10	44.25	43.86	41.07	43.96	42.64
Propan-2-ol	43.10	42.92	42.92	43.10	43.29	44.25	44.05	42.55	44.05	42.55
Methanol	42.92	42.74	42.92	42.92	44.44	43.29	44.05	40.98	44.05	42.55
Butan-1-ol	43.01	42.92	42.83	43.48	43.29	43.86	43.20	42.37	44.05	42.74
Propan-1-ol	42.92	42.74	41.67	43.29	43.29	44.64	44.44	41.32	44.05	42.55
Butan-2-ol	42.92	42.92	42.92	43.29	43.29	44.44	44.05	42.55	44.05	42.74
2-Methylpropan-2-ol	42.92	42.74	42.37	42.83	43.29	44.25	43.96	40.82	43.96	42.64
Tetrahydrofuran	41.67	41.67	42.92	41.75	41.84	42.49	42.50	40.98	42.02	41.67

TABLE II. Absorption frequencies ($\nu_{max}\times10^{-3}$ / cm^{-1}) for the higher wavelength peak of 3-[(4-substituted)phenylamino]isobenzofuran-1(3*H*)-ones in selected solvents

Solvent	Substituent									
	1	**2**	**3**	**4**	**5**	**6**	**7**	**8**	**9**	**10**
1,2-Dichloro-ethane	35.71	34.48	33.44	27.47	35.71	35.64	34.25	29.76	35.59	34.60
Decan-1-ol	35.97	35.97	32.89	33.61	35.71	32.63	32.41	29.41	35.46	35.84
Dichloromethane	35.84	35.65	33.67	34.48	35.71	35.71	34.36	30.03	35.59	35.59
1,4-Dioxane	35.97	35.84	34.01	33.11	35.78	34.31	34.07	29.24	35.59	34.60
Ethane-1,2-diol	35.46	35.46	33.44	34.59	35.40	33.50	31.75	27.06	32.47	35.40
Ethanol	36.76	35.71	33.44	35.71	35.59	33.90	33.00	28.82	35.46	34.13
Water	35.52	34.36	33.44	33.78	34.42	34.13	32.52	27.97	34.36	34.36
Hexane	36.10	36.07	33.44	35.34	34.25	34.07	34.78	31.20	35.84	35.21
2-Methylpropan--1-ol	35.91	35.91	33.61	33.44	35.91	34.25	32.95	29.24	35.59	34.42
Propan-2-ol	35.71	35.59	33.56	35.71	35.59	34.36	33.00	29.41	35.40	34.13
Methanol	35.84	35.71	33.44	33.44	35.84	33.67	33.22	29.07	35.46	34.13
Butan-1-ol	35.65	35.59	33.56	35.59	34.07	33.90	31.70	27.25	35.46	35.52
Propan-1-ol	35.59	34.13	33.44	35.59	35.53	33.56	32.89	29.07	35.46	34.13
Butan-2-ol	35.71	35.71	33.44	35.71	35.71	33.90	33.00	29.07	35.46	34.25
2-Methylpropan--2-ol	35.97	35.91	32.89	33.73	35.97	35.91	33.11	29.07	35.52	34.25
Tetrahydrofuran	34.48	34.36	33.67	33.44	34.25	34.25	33.84	29.24	34.36	34.19

From the results of the absorption maxima presented in Table I, it could be concluded that the first peak of 3-[(4-substituted)phenylamino]isobenzofuran-

1(3*H*)-ones is less sensitive to the substituent electronic effects and medium properties, although most of the electron-acceptor substituents (acetyl, nitro, fluoro and 2-pyridyl) induce a hypsochromic shift, when compared to the unsubstituted compound in all solvents. The introduction of an electron-donor substituent into the aryl part produces mostly a bathochromic shift except in some solvents, such as butan-1-ol, ethanol, ethane-1,2-diol, dioxane and tetrahydrofuran.

The absorption maxima of the second peak of 3-[(4-substituted)phenylamino]isobenzofuran-1(3*H*)-ones, positioned at longer wavelengths (Table II), showed bathochromic shift, compared to the unsubstituted compound **1** in all solvents. The introduction of electron-donor substituents into the arylidene part produces larger bathochromic shifts, suggesting a more pronounced intramolecular charge transfer (ICT) interaction in the molecule. On the other hand, the absorption maxima of 3-[(4-substituted)phenylamino]isobenzofuran-1(3*H*)-one derivatives showed a hypsochromic shift for all substances, and the largest was found for the nitro-substituted derivative (**8**).

The photophysical properties of molecules strongly depend on the molecular geometry, which could be observed as a result of the interplay of two factors: the stabilization of a molecule by the decoupling between donor and acceptor parts upon their twisting, and the resonance interaction leading to planarization of the molecule.[12] Both factors could be further influenced by the polarity of the solvent. In addition, the role of steric hindrance must be taken into account. The influence of the solvent on the absorption spectra is of particular importance since it is known that spectral behaviour of an organic molecule is strongly related to its electronic structure in both the ground and excited state.[12] The positions, intensities, and shapes of the absorption bands change as a result of physical intermolecular solute–solvent interaction forces (ion–dipole, dipole–dipole, dipole––induced dipole, hydrogen bonding, *etc*.), which primarily tend to alter the energy difference between ground and excited state of the absorbing species, containing the chromophore. Generally, the theories of solvent effects on absorption spectra assume that the chemical states of the isolated and solvated molecules are the same, and these effects are the consequence only as a physical perturbation of the relevant molecular states of the chromophores. Actually, a change of solvent is accompanied by variation of polarity, dielectric constant or polarizability of the surrounding medium, thus influencing the solvent interactions with ground and excited states of the molecule.[12] The bathochromic shift (positive solvatochromism) is associated with an increased solvent polarity, and it is caused by the significant difference in the charge distributions between the ground and excited state. The interaction of polar solvents is stronger with a more polar excited state. Therefore, a more polar excited state of a molecule is more stabilized in such a case, which leads to lower absorption energies, *i.e*., to larger bathochromic shifts.

Solvent effects on the UV–Vis absorption spectra: correlation with multi-parameter solvent polarity scales (LSER analysis)

The effect of various types of solvent–solute interactions on the shifts of the absorption maxima in sixteen solvents was also interpreted using the Kamlet–Taft and Catalán LSER models.[12–14] The LSER method was realised using the solvent parameters (Tables S-I and S-II) as independent variables and the absorption frequency as the dependant variable. The correlation analyses were performed using Microsoft Excel software at a confidence level of 95 %. The goodness of fit is discussed using the correlation coefficient (R), the standard error of the estimate (SE), and the Fisher significance test (F). The regression values v_0, s, a and b (Kamlet–Taft), and c, d, a and b (Catalán) fit, at the 95 % confidence level, are presented in Tables S-IV–S-VII, respectively.

The results in Tables S-IV–S-VII indicate that the solvent effects on the UV–Vis spectra are complex due to great diversity of both solvent and substituent effects. It could be noticed from the results given in Tables S-IV and S-V that, in most cases, the non-specific solvent effect is the factor contributing the most to the UV–Vis spectral shifts. The negative sign of coefficient s for the most compounds, except coefficient s for the first peak of compound **4** (Table S-IV) and for the second peak of compounds **3**, **5**–**7**, **9** and **10** (Table S-V), indicates a bathochromic (red) shift with increasing solvent dipolarity/polarizability. This suggests better stabilization of the excited electronic state relative to the ground state with increasing solvent polarity. The highest absolute values of coefficient s were found for compounds **6** and **8** for the lower wavelength peak and for compound **6** for the higher wavelength peak, which suggests better stabilization of the ground state relative to the excited state.

The results of the quantitative separation of the non-specific solvent effect into polarizability and dipolarity terms (coefficients c and d), performed using the Catalán equation, Eq. (2), are given in Tables S-VI and S-VII.

The results obtained using the Catalán equation provide better understanding of the attractive/repulsive solvent/solute interactions and enables an estimation of their appropriate contribution to the v_{max} shift in UV–Vis spectra. Comparison of the correlation results from Tables S-IV and S-V with the corresponding results from Tables S-VI and S-VII revealed that, in most cases, the correlation coefficients are more reliable on the Catalán scale, which highlights the importance of solvent polarizability (except for compound **6** for which the Catalán method gave a poor correlation with the exclusion of even 11 solvents). The correlation results, obtained according to Eq. (2) (Tables S-VI and S-VII), imply that the solvent polarizability is the principal factor influencing the shift of v_{max}, whereas the solvent dipolarity, acidity and basicity have moderate to low contributions. Negative values of the coefficient c, except for compounds **4** and **8** for the first peak and compound **10** for the second peak, indicate a higher contribution of the

polarizability effect to the stabilization of the excited state. Since the phthalide moiety acts as an electron-accepting group, the introduction of the substituents of different electronic properties causes variation in the mobility of the π-electrons, and thus, a wide range of coefficient *c* values were found. The effect of solvent dipolarity, designated by the *d* term, is of lower significance and showed complex behaviour, with the highest relative contribution for compounds **1** and **4**. Higher contribution of the solvent dipolar effect, in compounds with substituent displaying low/moderate effect, could be due to the balanced contribution of two opposing effects, *i.e.*, two distinct π-electronic entities, *i.e.*, the aryl and phthalide moieties, that cause separation of charges by creation of dipolar structures differently oriented in space.

Specific solvent–solute interactions realized through hydrogen bonding, *i.e.*, the HBD effect, could be attributed mainly to the carbonyl group of the phthalide moiety, lactone oxygen atom and nitrogen, while the solvent basicity HBA arises from the amino NH group. Negative values of the coefficient *a* found for both peaks, except for compounds **2**, **4**, **6**, **8** and **10**, indicate moderate to low contribution of the solvent acidity to the stabilization of the excited state.

Geometry optimization and TD-DFT calculations. Nature of the frontier molecular orbitals

The correlation results (Tables S-IV–S-VII) reflect different transmission modes of the electronic substituent effect. In this context, it was necessary to optimize the geometries of the investigated molecules. The 3-[(4-substituted)phenylamino]isobenzofuran-1(3*H*)-ones were fully optimized by the use of the DFT method. The atoms numbering and results of the energies of the optimized molecules by the DFT/B3LYP/6-31G(d,p) method are presented in Tables S-III and S-VIII, respectively, while the optimized structures in the gas phase are given in Fig. 2. Elements of the obtained optimized geometries of the investigated compounds are given in Table III. It was also found that the lactone product is more stable compared to open imine structure, given in Fig S-1, by approximately 14.7 kcal* mol^{-1}. In addition, the geometry of the investigated compounds was also calculated using the MP2 method and the results are presented in Table S-IX.

It could be seen that the geometric features of the studied 3-[(4-substituted)-phenylamino]isobenzofuran-1(3*H*)-ones follow a similar trend related to the geometry parameter change *versus* substituent effect. Taking into account the torsional angle (θ, Scheme 1), its change indicates that introduction of either strong electron-donating (methoxy or hydroxy) or electron-accepting substituents (acetyl, nitro or 2-pyridyl) increases the θ values, *i.e.*, increases deviation from planarity. In general, torsional angle (θ) change (83.44°) is the most pronounced when 2-pyridyl group is present in the molecule. The deviation from the planarity

* 1 kcal = 4184 J

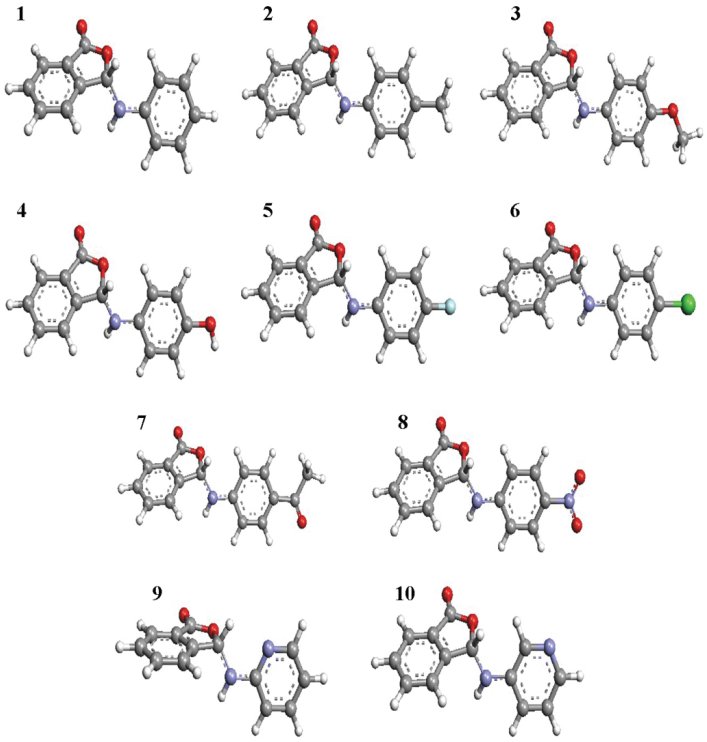

Fig. 2. Optimized structures of the 3-[(4-substituted)phenylamino]isobenzofuran-1(3*H*)-ones obtained using the DFT method.

increases with increasing electron-acceptor ability of the arylidene substituent. From the results in Table III, the introduction of electron-accepting substituent induces increases in the C1′–C2′, C3–N and C1–O2 bond lengths, while on the contrary, the N–C1′, C3–O2, C1=O, C1–C7a and N–H bond lengths decrease compared to the corresponding bonds in the unsubstituted molecule **1**. The opposite trend is exhibited when electron-donating substituents are present. A strong electron-accepting substituent supports an electron density shift to the phenyl ring from the rest of the molecule. The greater extent of the n,π-delocalization causes a decrease in the N–C1′ bond length, this part of the molecule acts as a separate unit. On the contrary, in the electron-donor substituted derivatives, the bond length of N–C1′, N–H, C3–O2, C1=O and C1–C7a are slightly longer, while the lengths of the C1′–C2′, C3–N and C1–O2 bonds decrease compared to those in the unsubstituted compound, giving rise to a greater contribution of electron delocalization from the phthalide unit. Moreover, the results of the molecule geometry optimization calculated using MP2/6-31G(d,p) method, given in Table S-IX, are in agreement with the results obtained using the DFT method.

TABLE III. Elements of the optimized geometries of the investigated, 3-[(4-substituted)phenylamino]isobenzofuran-1(3*H*)-ones **1**–**10** (Å) calculated by the DFT/6-31G(d,p) method

Cmpd.	C1–C7a	C1=O	C1–O2	C3–O2	C3–N	N–H	N–C1′	C1′–C2′	θ / °	μ / D*
1	1.4847	1.2057	1.3716	1.4777	1.4139	1.0115	1.4090	1.4047	69.86	4.804
2	1.4848	1.2059	1.3711	1.4793	1.4132	1.0117	1.4111	1.4042	69.62	4.688
3	1.4848	1.2060	1.3707	1.4820	1.4122	1.0121	1.4168	1.3989	69.92	5.476
4	1.4847	1.2060	1.3709	1.4818	1.4126	1.0123	1.4176	1.4011	69.75	5.668
5	1.4844	1.2054	1.3725	1.4777	1.4144	1.0119	1.4124	1.4045	69.16	5.358
6	1.4843	1.2050	1.3736	1.4744	1.4160	1.0115	1.4068	1.4046	69.12	5.867
7	1.4841	1.2046	1.3747	1.4703	1.4180	1.0110	1.3974	1.4092	70.14	5.724
8	1.4837	1.2036	1.3777	1.4648	1.4218	1.0108	1.3915	1.4103	70.31	8.799
9	1.4840	1.2060	1.3722	1.4693	1.4240	1.0111	1.3963	1.4084	83.44	5.139
10	1.4844	1.2048	1.3741	1.4719	1.4182	1.0120	1.4042	1.4022	69.53	6.500

The frontier molecular orbitals (FMOs) play an important role in optical and electric properties. The HOMO represents the ability to donate an electron and LUMO to obtain an electron; the HOMO–LUMO energy gap also determines the chemical reactivity and optical polarizability of a molecule. The frontier molecular orbital energies and energy gap between HOMO and LUMO orbitals of all compounds were calculated at the same level of theory and used to study the changes in the overall electronic distribution in the ground and excited states of the investigated molecules in gas phase, and the results are presented in Table IV. The plots of the calculated HOMO and LUMO molecular orbitals are presented in Table S-X. It could be noticed that the electron density of the HOMO orbitals for all molecules is mainly spread over the substituted phenyl ring, while the electron density for the LUMO orbitals is localized on the phthalide moiety. It could also be noted that the electron density of the LUMO orbital of the nitro--substituted molecule is considerably higher on the phenyl ring, due to the strong electron accepting character of the nitro-substituent, causing a π-electron density shift to the aryl moiety, regardless of the oppositely oriented, but weaker electron-accepting character of the phthalide moiety. Generally, the E_{gap} values were lower for molecules with electron-donor substituents and higher for compounds with electron-acceptor substituted molecules (except nitro substituted compound **8**) in comparison to the unsubstituted molecule **1**. The larger energy gap in the gas phase, found for the electron-acceptor substituted compounds **7**, **9** and **10** is a consequence of significant stabilization of the HOMO orbitals. Considering the results of geometry optimization from Table III, it is clear that these are compounds with more pronounced deviation from planarity. In addition, as could be seen in Table IV, the calculated HOMO and LUMO energies in methanol are slightly lower than those in the gas phase. The lowest energy gap in gas phase was observed for the molecule with a methoxy substituent (**3**) and the highest for

* 1 D = 3.33564×10^{-30} C m

the compound containing a 2-pyridyl group (**9**) in both the gas phase and the solvent methanol.

TABLE IV. Calculated energies of the HOMO and LUMO orbitals and energy gaps for investigated compounds **1**–**10** by the TD-DFT/6-31G(d,p) method in gas phase and the solvent methanol

Molecule	Gas			Methanol		
	E_{HOMO} / eV	E_{LUMO} / eV	E_{gap} / eV	E_{HOMO} / eV	E_{LUMO} / eV	E_{gap} / eV
1	–5.811	–1.439	4.372	–6.105	–1.709	4.396
2	–5.643	–1.407	4.236	–5.934	–1.699	4.235
3	–5.354	–1.375	3.979	–5.678	–1.690	3.988
4	–5.426	–1.391	4.036	–5.714	–1.690	4.024
5	–5.840	–1.499	4.341	–6.098	–1.718	4.380
6	–5.928	–1.563	4.365	–6.157	–1.735	4.422
7	–6.081	–1.625	4.456	–6.305	–1.759	4.546
8	–6.521	–2.150	4.371	–6.590	–2.604	3.986
9	–6.104	–1.327	4.777	–6.326	–1.685	4.641
10	–6.132	–1.547	4.584	–6.362	–1.742	4.620

In order to gain a better understanding of the energetic behaviour of molecules, additional TD-DFT calculations including solvent influence in the solvent methanol were performed with the CAM-B3LYP long range-corrected functional[15] and the 6-31G(d,p) basis set. The solvent in the TD-DFT calculations was simulated with the polarizable continuum model (PCM). TD-DFT provides a good benchmark in the determination of spectroscopic properties due to the accurate description of ground and excited potential energy surfaces. The calculated vertical excitation energies, oscillator strength (*f*) and the composition of the most significant singlet excited states are shown in Table V. The presented results for the electronic transitions also indicate that the compounds show bathochromic shifts compared to the unsubstituted compound in the solvent methanol (except **5** and **9**), and the lowest frequency is observed for the nitro-substituted compound. These results are consistent with experimental ones (Table II). Furthermore, it is evident that only the absorption for compound **8** originates from a pure HOMO–LUMO transition (98.1 %), while for the other compounds different transitions are included, *e.g.*, HOMO→LUMO+3 for compounds **1**–**4**, **6**, **9** and **10**, HOMO–3→LUMO for compound **5** and HOMO→LUMO+1 for compound **7**. The molecular orbital surfaces of the orbitals included in the electronic transitions and their energies in solvent methanol for all compounds are presented in Fig. 3.

Comparing the calculated TD-DFT results to the experimental ones in Table VI for methanol, it is obvious that there is a good agreement between the calculated and experimental values. From experimental and calculated absorption frequency results in methanol, it could be concluded that the nitro-substituted com-

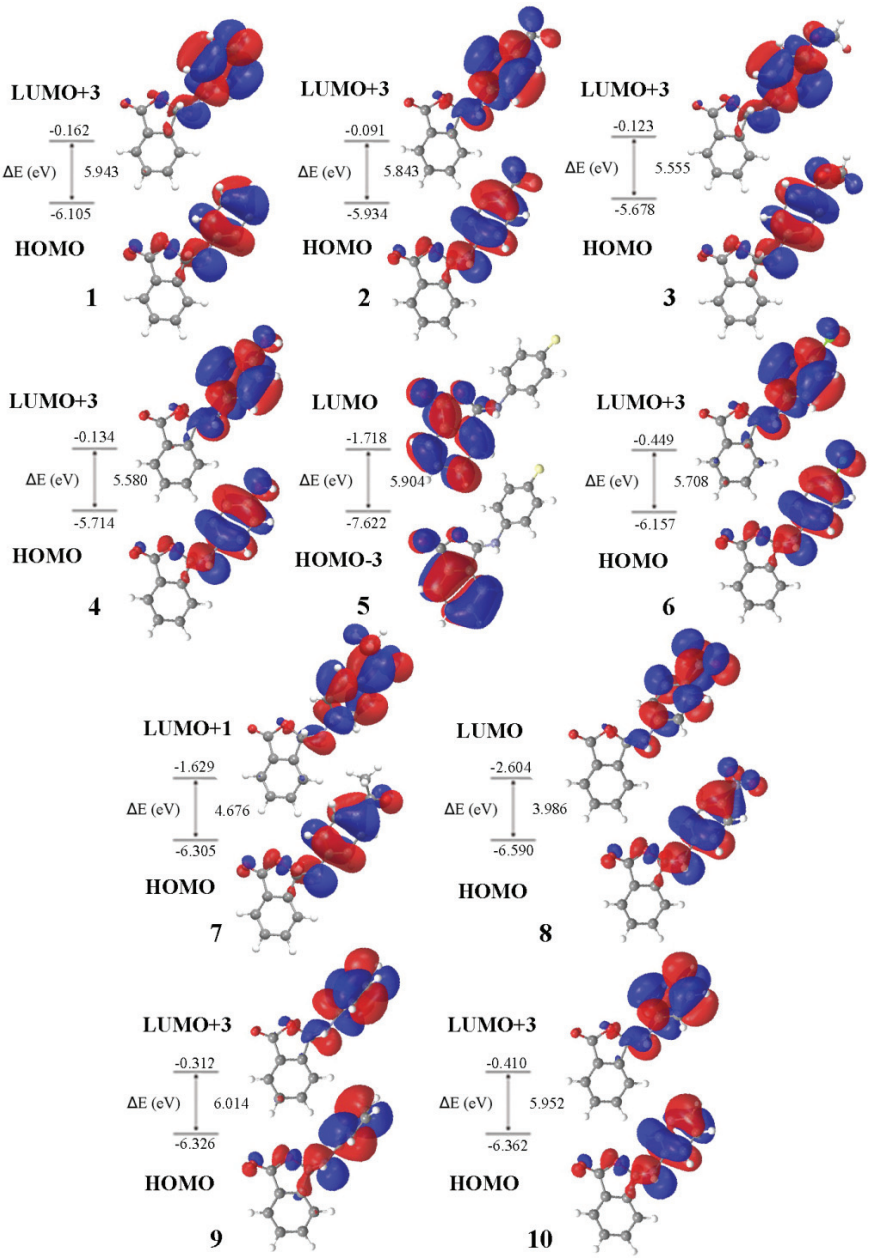

Fig. 3. The main transitions and corresponding orbitals for compounds **1**–**10** in the solvent methanol calculated by the TD-DFT method.

pound **8** showed the most pronounced bathochromic effect with respect to the unsubstituted compound **1**. However, the calculated frequencies are somewhat

higher compared to the corresponding experimental values, but it is already known in the literature that this method overestimates the energies of electronic transitions.[22]

TABLE V. Calculated excitation energy (E_{exc}), oscillator strength (f), configuration interaction (CI) expansion coefficient and percentage of single particle excitation contribution for the most significant singlet excited states for compounds **1**–**10** in the solvent methanol calculated by the TD-DFT method

Comp.	E_{exc} / eV	f	Excitation	CI expansion coefficient	Single particle excitation contribution, %
1	5.4640	0.4417	HOMO → LUMO+3	0.52237	54.6
			HOMO–3 → LUMO	–0.40185	32.3
			HOMO–1 → LUMO+2	0.14225	4.05
2	5.3915	0.5588	HOMO → LUMO+3	0.65413	85.6
			HOMO–1 → LUMO+2	–0.17583	6.2
			HOMO–3 → LUMO	0.14079	4.0
3	5.3529	0.5687	HOMO → LUMO+3	0.65988	87.1
			HOMO–1 → LUMO+2	0.16845	5.7
			HOMO–3 → LUMO	–0.10535	2.2
4	5.4258	0.4955	HOMO → LUMO+3	0.63097	79.6
			HOMO–3 → LUMO	0.20609	8.5
			HOMO–1 → LUMO+2	–0.17098	5.8
5	5.4795	0.2973	HOMO–3 → LUMO	0.58891	69.4
			HOMO → LUMO+3	0.28121	15.8
			HOMO–2 → LUMO+1	–0.17924	6.4
			HOMO–2 → LUMO	0.10049	2.0
6	5.2732	0.4984	HOMO → LUMO+3	0.61157	74.8
			HOMO–1 → LUMO	–0.25540	13.0
			HOMO-1 → LUMO+2	–0.13776	3.8
			HOMO–2 → LUMO	0.13393	3.6
7	4.3448	0.6927	HOMO → LUMO+1	0.69485	96.6
8	3.6795	0.5252	HOMO → LUMO	0.70047	98.1
9	5.5950	0.3675	HOMO → LUMO+3	0.62228	77.4
			HOMO–1 → LUMO+3	0.17793	6.3
			HOMO–2 → LUMO	–0.16060	5.2
			HOMO–5 → LUMO+1	0.12682	3.2
			HOMO–3 → LUMO+2	0.10946	2.4
10	5.4044	0.3091	HOMO → LUMO+3	0.55575	61.8
			HOMO–1 → LUMO+3	–0.35925	25.8
			HOMO–3 → LUMO	0.15478	4.8
			HOMO–4 → LUMO+1	0.10941	2.4

The experimental and theoretical studies indicate that the solvatochromic and physicochemical properties of the studied phthalides are the consequence of the overall effect of the molecule geometry, influenced by the effects of electronic substituents transmitted through the π-conjugated systems and the results obtained in this study could help in assessing potential applications of the inves-

tigated compounds. Such results could be useful in designing new biologically active compounds allowing an estimation of the site of electrophilic or nucleophilic attacks in some photochemical reactions. The obtained results could also be significant in QSAR or QSPR studies in the evaluation of their biological activity.

TABLE VI. Experimental absorption frequencies and those calculated by TD-DFT method in the solvent methanol

Molecule	$\nu_{1calc}\times10^{-3}$ / cm^{-1}	$\nu_{1exp}\times10^{-3}$ / cm^{-1}	$\nu_{2calc}\times10^{-3}$ / cm^{-1}	$\nu_{2exp}\times10^{-3}$ / cm^{-1}
1	44.07	42.92	39.39	35.84
2	43.49	42.74	38.50	35.71
3	43.17	42.92	36.44	33.44
4	43.76	42.92	36.63	33.44
5	44.19	44.44	38.04	35.84
6	42.53	43.29	36.82	33.67
7	43.61	44.05	35.04	33.22
8	39.76	40.98	29.68	29.07
9	45.13	44.05	37.82	35.46
10	43.59	42.55	37.36	34.13

CONCLUSIONS

The substituent and solvent effects on the shifts of the UV–Vis absorption maxima of 3-[(4-substituted)phenylamino]isobenzofuran-1(3*H*)-ones were successfully evaluated, based on experimental data and theoretical calculations. The results showed that the absorption maxima are more dependent on the substituent than on the solvent effect. Solvent polarizability is the principal factor that influences the shift of the absorption maxima, whereas the solvent dipolarity, acidity and basicity are of lower importance. The absorption maxima undergo a bathochromic shift with increasing solvent polarizability, indicating that the excited state is more polarisable than the ground state. Specific interactions through hydrogen bonding, expressed by the solvent acidity and basicity, could be attributed mainly to the carbonyl and amino moieties, and it is slightly affected by the substituent present in the aryl part.

The optimized geometries of the investigated compounds showed that introduction of either strong electron-donating (methoxy or hydroxy), or electron-accepting substituents (acetyl, nitro or 2-pyridyl) increases the θ values, *i.e.*, increases the deviation from planarity. In general, the torsion angle (θ) change (83.44°) is the most pronounced when a 2-pyridyl group is present in the molecule.

Generally, in comparison with unsubstituted molecule **1**, the E_{gap} values were lower for molecules with electron-donating substituents and higher for compounds with electron-accepting supstituents. The lowest energy gap in the gas phase was observed for the compound with a methoxy substituent (**3**) and the highest for the compound containing a 2-pyridyl group (**9**). It could be noticed

that the electron densities of the HOMO orbitals for all molecules are dominantly populated on the substituted phenyl ring, while the electron density for the LUMO orbitals are populated on the phthalide moiety (except for the nitro-substituted compound). However, it is evident from the TD-DFT results that only the absorption for the compound **8** originates from a pure HOMO–LUMO transition (98.1 %), while for the other compounds, other transitions are included, *e.g.*, HOMO→LUMO+3, HOMO–3→LUMO or HOMO→LUMO+1. Results of the TD-DFT calculations in methanol as a solvent showed the good agreement of the calculated and experimental frequencies.

SUPPLEMENTARY MATERIAL

Solvent parameters and results of characterization are available electronically at the pages of the Journal website: http://www.shd.org.rs/JSCS/, or from the corresponding author on request.

Acknowledgement. This work was supported by the Ministry of Education, Science and Technological Development of the Republic of Serbia (Project No. 172013).

ИЗВОД

ЕКСПЕРИМЕНТАЛНО И ТЕОРИЈСКО ПРОУЧАВАЊЕ УТИЦАЈА РАСТВАРАЧА И СУПСТИТУЕНАТА НА УНУТАРМОЛЕКУЛСКУ ПРОМЕНУ НАЕЛЕКТРИСАЊА КОД 3-[(4-СУПСТИТУИСАНИХ)ФЕНИЛАМИНО]ИЗОБЕНЗОФУРАН-1(3*H*)-ОНА

НЕВЕНА ПРЛАИНОВИЋ[1], МИЛИЦА РАНЧИЋ[2], ИВАНА СТОЈИЉКОВИЋ[2], ЈАСМИНА НИКОЛИЋ[3], САША ДРМАНИЋ[3], ISMAIL AJAJ[4] и АЛЕКСАНДАР МАРИНКОВИЋ[3]

[1]*Иновациони центар Технолошко–металуршког факултета, Универзитет у Београду, Карнегијева 4, 11120 Београд,* [2]*Шумарски факултет, Универзитет у Београду, Кнеза Вишеслава 1, 11030 Београд,* [3]*Технолошко–металуршки факултет, Универзитет у Београду, Карнегијева 4, 11120 Београд и* [4]*Faculty of Arts and Science, The university of El-Margeb, Mesallata, Libya*

Утицај супституената и растварача на солватохромизам код 3-[(4-супституисаних)-фениламино]изобензофуран-1(3*H*)-она је проучаван експерименталном и теоријском методологијом. Утицаји специфичних и неспецифичних интеракција између молекула растварача и испитиваних једињења на померања UV–Vis апсорпционих максимума су процењени помоћу једначина Камлет–Тафта и Каталана. Експериментални резултати су тумачени помоћу DFT и TD-DFT метода. HOMO/LUMO енергије ($E_{\mathrm{HOMO}}/E_{\mathrm{LUMO}}$), њихове разлике ($E_{\mathrm{gap}}$),као и механизам побуђивања електона и промене расподеле електронске густине и у основном и у побуђеном стању испитиваних једињења, проучавани су израчунавањем у гасној фази. Електронски прелази су израчунати TD-DFT методом у метанолу као растварачу. Утврђено је да и супституенти и растварачи утичу на промену електронске густине, тј. на величину конјугације и на унутармолекулску промену наелектрисања.

(Примљено 8. априла, ревидирано 28. новембра, прихваћено 7. децембра 2017)

REFERENCES

1. G. Lin, S. S.-K. Chan, H.-S. Chung, S.-L. Li, *Stud. Nat. Prod. Chem.* **32** (2005) 611
2. R. Karmakar, P. Pahari, D. Mal, *Chem. Rev.* **114** (2014) 6213
3. Y.-Q. Zhu, J.-X. Li, T.-F. Han, J.-L. He, K. Zhu, *Eur. J. Org. Chem.* **2017** (2017) 806

4. T. Saito, T. Itabashi, D. Wakana, H, Takeda, T. Yaguchi, K. Kawai, T. Hosoe, *J. Antibiot.* **69** (2016) 89
5. R. A. Limaye, V. B. Kumbhar, A. D. Natu, M. V. Paradkar, V. S. Honmore, R. R. Chauhan, S. P. Gample, D. Sarkar, *Bioorg. Med. Chem. Lett.* **23** (2013) 711
6. G. Strobel, E. Ford, J. Worapong, J. K. Harper, A. M. Arif, D. M. Grant, P. C. W. Fung, R. M. W. Chau, *Phytochemistry* **60** (2002) 179
7. S. F. Brady, M. M. Wagenaar, M. P. Sing, J. E. Janso, *Org. Lett.* **2** (2000) 4043
8. T. H. Chou, I. S. Chen, T. L. Hwang, T. C. Wang, T. H. Lee, L. Y. Cheng, Y. C. Chang, J. Y. J. Y. Cho, J. J. Chen, *J. Nat. Prod.* **71** (2008) 1692
9. L. P. L. Lograd o, C. O. Santos, L. A. S. Romeiro, A. M. Costa, J. R. O. Ferreira, B. C. Cavalcanti, O. M. de Moraes, L. V. Costa-Lotufo, C. Pessoa, M. L. dos Santos, *Eur. J. Med. Chem.* **45** (2010) 3480
10. M. Rančić, N. Trišović, M. Milčić, G. Uščumlić, A. Marinković, *Spectrochim. Acta, A* **86** (2012) 500
11. A. Sarkar, P. Banerjee, S. U. Hossain, S. Bhattacharya, S. C. Bhattacharya, *Spectrochim. Acta, A* **72** (2009) 1097
12. C. Reichardt, *Solvents and Solvent Effects in Organic Chemistry*, 3rd ed., Wiley–VCH, Weinheim, 2003, p. 432
13. M. J. Kamlet, J. L. M. Abboud, R. W. Taft, *An examination of linear solvation energy relationships*, in *Progress in Physical Organic Chemistry,* vol. 13, R. W. Taft, Ed., Wiley, New York, 1981, p. 485
14. J. Catalán, *J. Phys. Chem., B* **113** (2009) 5951
15. T. Yanai, D. Tew, N. Handy, *Chem. Phys. Lett.* **393** (2004) 51
16. *Gaussian 09, revision C.01*, Gaussian Inc., 2009, Wallingford, CT
17. A. Amer, H. Zimmer, *J. Heterocyclic Chem.* **18** (1981) 1625
18. S. N. Khattab, S. Y. Hassan, A. El-Faham, A. M. M. El Massry, A. Amer, *J. Heterocyc. Chem.* **44** (2007) 617
19. M. S. Masoud, R. M. I. Elsamra, S. S. Hemdan, *J. Serb. Chem. Soc.* **82** (2017) 851
20. M. Faraji, A. Farajtabar, *J. Serb. Chem. Soc.* **81** (2016) 1161
21. D. R. Brkić, J. B. Nikolić, A. R. Božić, V. D. Nikolić, A. D. Marinković, H. Elshaflu, S. Ž. Drmanić, *J. Serb. Chem. Soc.* **81** (2016) 979
22. D. Jacquemin, A. Planchat, C. Adamo, B. Mennucci, *J. Chem. Theory Comput.* **8** (2012) 2359.